Properties of Connexin 46 Hemichannels in Dissociated Lens Fiber Cells

Lisa Ebihara,[1] *Jun-Jie Tong,*[1] *Barbara Vertel,*[2] *Thomas W. White,*[3] *and Tung-Ling Chen*[1]

Purpose. To characterize the properties of connexin 46 hemichannels in differentiating fiber cells isolated from mouse lenses.

Methods. Differentiating fiber cells were isolated from mouse lenses using collagenase. Cellular localization of connexin 50 (Cx50) and connexin 46 (Cx46) was assessed by immunofluorescence. Membrane currents were recorded using whole cell patch clamping. Dye uptake was measured using time-lapse imaging.

Results. In freshly dissociated fiber cells isolated from knockout Cx50 (KOCx50) mouse lenses, removal of external divalent cations induced a macroscopic current composed of large conductance channels. This current was reduced at a holding potential of −60 mV, activated on depolarization, and had a reversal potential near 0 mV. These properties were very similar to those of Cx46 hemichannel currents recorded in single *Xenopus* oocytes. If the currents observed in divalent cation-free Ringer's solution were due to Cx46 hemichannel opening, then dye influx by gap junctional/hemichannel permeable dyes should be measurable in the fiber cells. To measure dye influx, the authors used the positively charged dyes, propidium iodide (PrI) and 4′-6-diamidino-2-phenylindole (DAPI). In the absence of external calcium, fiber cells took up both dyes. Furthermore, dye influx could be inhibited by hemichannel blockers. To confirm that this current was due to Cx46 hemichannels, the authors studied fiber cells isolated from the lenses of double knockout ($Cx46^{-/-}$; $Cx50^{-/-}$) mice and demonstrated that both the calcium-sensitive conductance and dye influx were absent.

Conclusions. These results show that Cx46 can form functional hemichannels in the nonjunctional membrane of fiber cells. (*Invest Ophthalmol Vis Sci.* 2011;52:882–889) DOI:10.1167/iovs.10-6200

Gap junctions are membrane specializations containing intercellular channels that allow the passage of ions and small metabolites between neighboring cells. These channels are made up of protein subunits called connexins, which are members of a multigene family with at least 20 human members.[1] A gap junctional hemichannel, or connexon, is an oligomeric protein composed of six connexins. Two connexons from neighboring cells dock to form a gap junctional channel. During gap junction channel formation, connexons traffic to the nonjunctional plasma membrane, where they reside as functional hemichannels before assembling into gap junctional channels (reviewed in Ref. 2). These hemichannels are usually closed at negative resting potentials. However, they can be activated in response to certain stimuli such as depolarization or reduction in external calcium concentration.[3–5]

Cx46 is a gap junctional protein that is expressed at high levels in lens fiber cells along with Cx50.[6,7] The importance of this protein in maintaining lens transparency has been demonstrated by the observation that mutations in Cx46 produce cataracts in humans and mice.[8–10] Furthermore, genetically engineered mice deficient in Cx46 develop severe cataracts that are associated with a partial loss of coupling of the differentiating fibers and a complete loss of gap junctional coupling of the mature fiber cells.[11,12]

The functional properties of gap junctional channels and hemichannels formed by Cx46 have been characterized in exogenous expression systems such as *Xenopus* oocytes and communication-deficient mammalian cell lines.[4,6,13–22] These studies show that Cx46 not only forms gap junctional channels but also forms functional hemichannels in the nonjunctional plasma membrane of single oocytes. The hemichannels close over a narrow range of calcium concentrations (1–2 mM) when held at a membrane potential of −10 mV.

Evidence for the presence of connexin hemichannels in lens fiber cells came from a study by Rae et al.[23] who showed that removal of extracellular divalent cations resulted in a decrease in resting membrane potential and a large increase in input conductance of the intact lens. These effects were originally attributed to activation of a stretch activated, nonselective cation channel, but another possibility is that they were due to Cx46 and Cx50 hemichannels whose probability of opening is increased in low $[Ca^{2+}]_o$.[4] Further evidence for the presence of connexin hemichannels in the lens came from a study by Eckert et al.[24] who identified a large, nonselective current in isolated fiber cells that resembled the membrane currents recorded from *Xenopus* oocytes injected with cRNA for rat Cx46.[4]

Recently, our laboratory developed a technique for producing a viable, isolated mouse fiber cell preparation. This preparation is amendable to electrophysiological analysis using patch clamp recording techniques. In the present study, we used freshly isolated fiber cells that were deficient in Cx50 to study the properties of Cx46 hemichannels.

Methods

Mouse Breeding

KOCx50 mice[25] were interbred with KOCx46 mice[11] to produce KOCx50-KOCx46 animals. Genomic DNAs isolated from tail biopsies were genotyped by polymerase chain reaction (PCR) using previously described protocols.[11,25,26]

From the Departments of [1]Physiology and Biophysics, and [2]Anatomy and Cell Biology, Rosalind Franklin School of Medicine and Science, North Chicago, Illinois; and the [3]Department of Physiology, SUNY at Stony Brook, Stony Brook, New York.

Supported by National Institutes of Health Grants RO1 EY10589 (LE) and R01 EY13163 (TWW).

Submitted for publication July 12, 2010; revised August 20, 2010; accepted August 21, 2010.

Disclosure: **L. Ebihara**, None; **J-J. Tong**, None; **B. Vertel**, None; **T.W. White**, None; **T-L. Chen**, None

Corresponding author: Lisa Ebihara, Department of Physiology and Biophysics, Rosalind Franklin University of Medicine and Science, 3333 Green Bay Rd., North Chicago, IL 60064; lisa.ebihara@rosalindfranklin.edu.

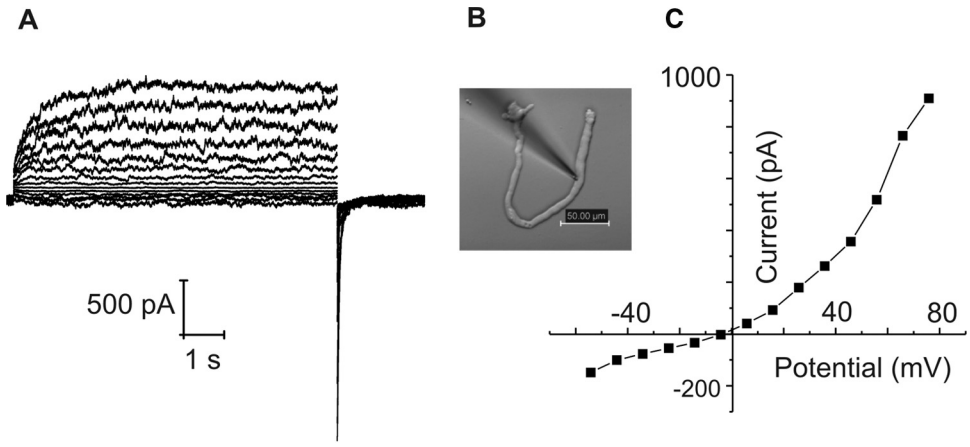

FIGURE 1. Membrane currents in a KOCx50 fiber cell. (**A**) A family of current traces was recorded from the fiber cell shown in (**B**) using the whole cell patch clamp technique. A series of depolarizing steps was applied in 10 mV increments between −60 and 80 mV from a holding potential of −80 mV. (**C**) I–V relations obtained from the data shown in (**A**). The current was measured at the end of the 8-second pulse and plotted as a function of voltage after correction for liquid junction potential.

Dissociation of Differentiating Lens Fiber Cells

Mice (4–5 weeks old) were killed by CO_2 asphyxiation and cervical dislocation in accordance with protocols approved by the Rosalind Franklin University Animal Care and Use Committee and in accordance with the ARVO Statement for the Use of Animals in Ophthalmic and Vision Research. The lenses were dissected free from the extracted eyes and placed in dissociation buffer (DB, in mM: 170 NaGluconate, 4.7 KCl, 5 glucose, 5 HEPES, pH 7.4). Adherent non-lens material was carefully removed from the lens with a pair of forceps. A posterior tear was made in the lens capsule and the capsule was removed. The epithelial cells and strands of elongating fiber cells remained attached to the capsule. The capsule and adherent epithelial and fiber cells were incubated in DB containing 0.125% collagenase (Type IV, Worthington Biochemical, Lakewood, NJ) and 0.5% protease (type XXIV, Sigma-Aldrich, St. Louis, MO) at room temperature for 15 to 30 minutes. Then the capsule was resuspended in DB containing TrpLE (Invitrogen Life Technologies, Carlsbad, CA) and incubated for an additional 1 to 2 minutes. The capsule was washed once with DB and resuspended in DB. The epithelial and young fiber cells were removed from the capsule by gentle trituration with a fire-polished Pasteur pipette. The cells were then pelleted (1000*g* for 2 minutes) and resuspended in DB. The isolated cells were used immediately for patch clamp and imaging experiments.

An alternative procedure for dissociating fiber cells involved treating the capsule with DB containing 0.125% collagenase (Type IV, Worthington Biochemical) and 0.5% protease (type XXIV, Sigma-Aldrich) at 37°C for 12 to 30 minutes, then resuspending the capsule in DB containing 0.125% collagenase and incubated for an additional 10 minutes at room temperature.

Immunofluorescence Localization

Dissociated lens (fiber) cells were collected on collagen-coated glass coverslips, fixed in iced methanol at −20°C for 10 minutes and stored at −4°C before immunostaining. Cells on coverslips were re-equilibrated in phosphate-buffered saline (PBS), pre-incubated in 30% normal serum (goat or donkey) for 25 minutes at room temperature and incubated in primary antibodies for 2½ hours at 37°C. Six washes in PBS over 30 minutes were followed by incubation in fluorophore-conjugated secondary antibody IgGs for 1 hour at 37°C. After six washes in PBS over 45 minutes, immunostained specimens were mounted in antifade reagent with DAPI (Prolong Gold, Invitrogen) and left overnight in the dark. Specimens were observed and images captured using a microscope (Leica DMRB; Leica Microsystems, Wetzlar, Germany) equipped with a camera (Hamamatsu CCD; Hamamatsu, Bridgewater, NJ) and imaging software (Openlab; Improvision, Coventry, England).

The following antibodies were used: mouse monoclonal IgM directed against connexin 50 (Zymed; Zymed Laboratories, San Francisco, CA), rabbit polyclonal antibodies for connexin 46 (Alpha Diagnostic International, San Antonio, TX), Fluorescence-labeled secondary antibodies were purchased from Jackson ImmunoResearch (West Grove, PA) and included FITC goat anti-mouse IgM and donkey anti-rabbit IgG (DyLight 594, Jackson Immunoresearch).

Electrophysiological Recording and Analysis

Membrane currents were recorded in dissociated fiber cells using the whole cell patch clamp technique. A collagen-coated, glass bottom tissue culture dish (MatTek, Ashland, MA) was used as the recording

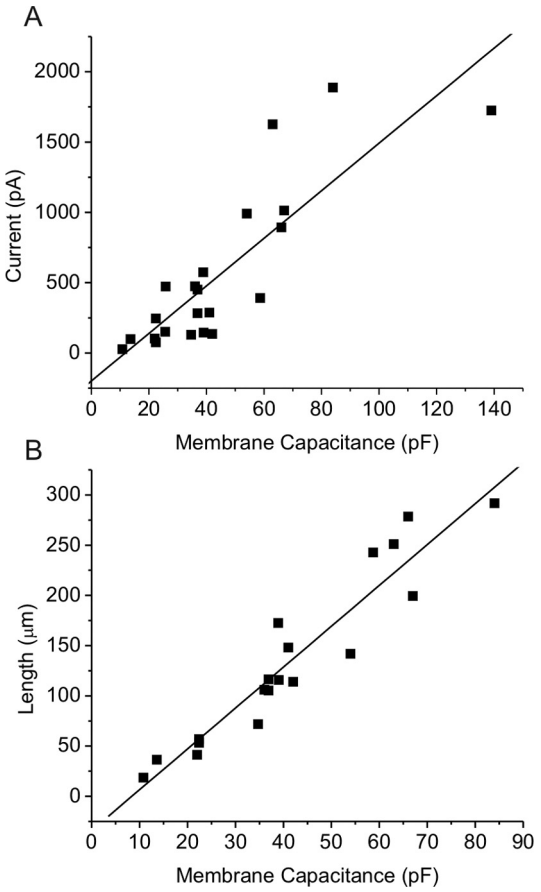

FIGURE 2. The amplitude of the hemichannel current is linearly correlated to membrane capacitance. (**A**) Steady state current amplitude (measured at the end of an 8-second pulse to 30 mV) is plotted as a function of membrane capacitance. $n = 22$. (**B**) Plot of cell length versus membrane capacitance for same data set shown in (**A**).

chamber. Only fiber cells that appeared to be healthy based on morphologic criteria and tightly adherent to the bottom of the recording chamber were used for experiments. A computer-controlled patch clamp amplifier (MultiClamp 700A, Molecular Devices, Sunnyvale, CA) was used to control membrane potential and measure membrane current. The resistance of the patch pipettes was 2 to 6 mΩ when filled with standard internal solution. The internal solution contained (in mM): 150 CsCl, 10 EGTA, 0.5 $CaCl_2$, 3 MgATP, 2 Na_2ATP, 10 HEPES-Na, pH 7.4, osmolarity 310 to 320 mOsm. The standard extracellular solution was divalent cation-free NaGluconate Ringer's which contained (in mM): 150 NaGluconate, 4.7 KCl, 5 glucose, 5 HEPES, pH 7.4, osmolarity 310 to 320 mOsm. The osmolarity was measured using a vapor pressure osmometer (Wescor, Logan, UT). The patch pipette was positioned on the cell with a piezoelectric micromanipulator (Burleigh PCS-5000; Exfo Life Sciences, Mississauga, Ontario, Canada). Pulse generation and data acquisition were performed using a PC computer equipped with commercial software (PCLAMP 9.2; Molecular Devices) and an acquisition system (Digidata 1320A; Molecular Devices). The cell was focally perfused with drugs using a millimanifold applicator (ALA Scientific, Farmingdale, NY) whose tip was brought near and pointed at the cell of study using a manipulator. Using this system, solutions flowing over the cell could be changed within a few seconds. The bath was grounded via a 1 mm diameter silver wire electrode mounted in a pipette tip filled with 3M KCl agar. Images of fiber cells were acquired via a cooled CCD camera (Coolsnap ES2, Photometrics; Roper Scientific, Tucson, AZ) driven by an imaging program (Nikon Elements; Nikon Instruments, Melville, NY). All the experiments were conducted at room temperature (21–24°C). Data were analyzed using three different programs (PCLAMP 9.2 [Molecular Devices], SigmaPlot 11 [Systat Software, Chicago, IL], and OriginPro 8 [OriginLab, Northhampton, MA]).

All the membrane potentials in the graphs were corrected for liquid-junction potentials after the experiment using the "junction potential calculator" interface (Clampex version 9.2; Molecular Devices). The voltage clamp protocols were not corrected for the liquid junction potential. They represent the command potentials that were applied to the patch pipette.

Instantaneous I–V curves were determined by measuring the isochronal tail currents. Ionic currents were evoked by pulsing from a holding potential of −60 mV to +80 mV for 1.5 seconds and then hyperpolarizing to different test potentials. Tail current amplitudes were determined at isochronal points ranging from 4 to 10 ms after repolarization. The exact time at which the tail current amplitude was measured depended on the time required for the capacitive transient to decay to a value close to zero.

Fluorescence Imaging

Dissociated lens fibers in 150 μL of DB were placed on a collagen-coated glass bottom culture dish (MatTek, Ashland, MA) for 15 minutes allowing the fibers to attach. The dish was then fitted with a closed bath insert (RC-37FC; Warner Instruments) connected to perfusion reservoirs and perfused with NaGluconate Ringer's solution. The whole device was then mounted on an inverted microscope (Nikon TE2000; Nikon Instruments) outfitted with a motorized microscope stage (Prior ProScan; Molecular Devices) controlled by imaging software (Metamorph Imaging; Molecular Devices) and imaged with a 20 × 0.75 NA objective (Plan-Apochromat; Nikon Instruments). After the fields with fiber cells were selected and registered in the imaging system, and 2 mL of NaGluconate Ringer's solution containing 2 μM PrI and 2 μM DAPI were perfused through the device, image capturing was initiated at 2-minute intervals using a cooled CCD camera (Cascade 512B; Roper Scientific). Filter combinations for excitation/emission were set at 360/465 for DAPI and 572/630 for PrI. At specified times, perfusion of NaGluconate Ringer's solution containing desired inhibitors was performed, and images were captured as previously.

The fluorescence intensity was measured (Metamorph Imaging software; Molecular Devices). For each fiber cell measured, a region covering a representative area in the fiber cell and another region outside the cells to represent the background were measured. The values were exported to Excel for analysis. The corrected intensity at each time point was generated by subtracting the background intensity from fluorescence intensity in fiber cells.

Results

We isolated single fiber cells and small groups of fiber cells from 4 to 5 week old KOCx50 mouse lenses. The fiber cells ranged between 15 to 400 μm in length. Most of these cells still contained nuclei that could be visualized using DAPI indicating that they were from the outer cortex. Some of these cells adhered to the bottom of a tissue culture dish and could be

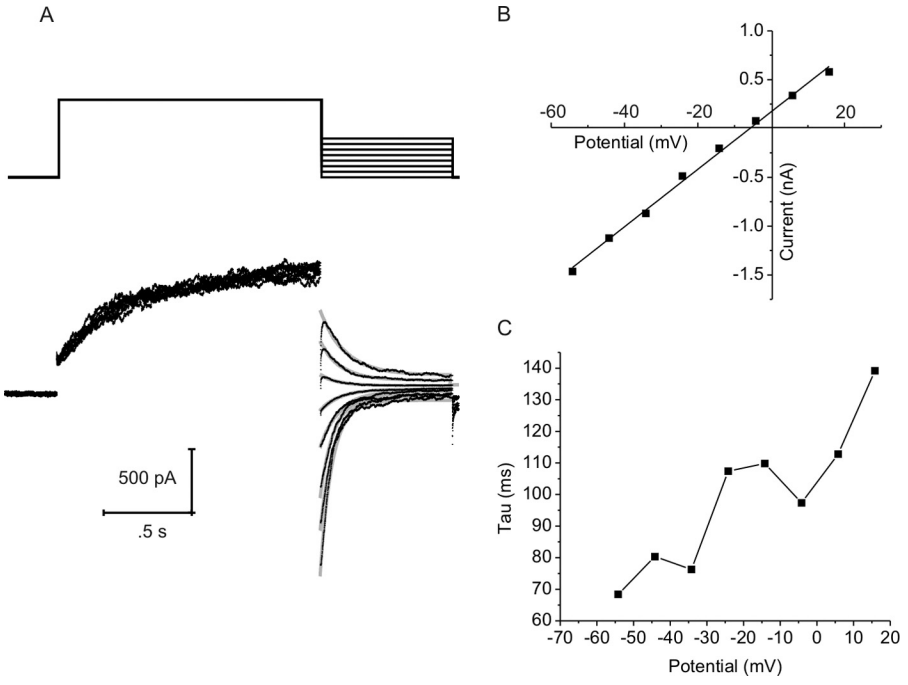

Figure 3. (**A**) A family of whole cell tail currents recorded from a lens fiber cell. The voltage clamp protocol is shown. The voltage was stepped from a holding potential of −60 mV to 80 mV for 1.5 seconds to open the hemichannels and then repolarized to voltages between −60 and +10 mV. (**B**) Instantaneous I–V relationship determined by measuring the isochronal tail currents. Continuous line represents the best fit of the instantaneous I–V relationship to a linear regression. (**C**) Time constants of deactivation plotted as a function of voltage. The time constants of deactivation were obtained by fitting the time course of deactivation of the tail currents shown in (**A**) to a single exponential (*solid light gray lines*).

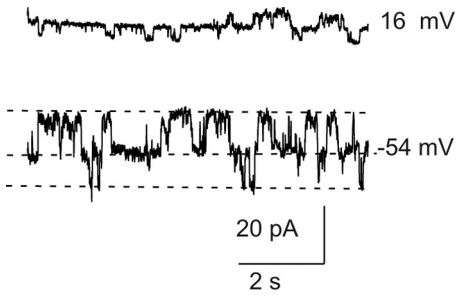

FIGURE 4. Whole cell current traces recorded from a small fiber in response to voltage clamp steps to the indicated potentials from a holding potential of −60 mV. The whole cell current shows discrete steps indicative of opening and closing of single hemichannels. The fiber cell had a length ~20 μm, based on its membrane capacitance of 13.2 pF.

maintained in divalent cation-free Ringer's solution in which chloride had been replaced by gluconate for several hours. These cells were viable when assessed using the LIVE/DEAD assay (Invitrogen), which tests for intracellular esterase activity and ethidium homodimer exclusion in viable cells (data not shown).

We have used this preparation to characterize Cx46 hemichannels. Membrane currents were recorded in whole cell patch clamp mode. To minimize contamination by chloride and potassium channels, divalent cation-free NaGluconate Ringer's was used as the bath solution and the pipette solution was filled with CsCl internal solution. Under these conditions, the main current in the cells was a time- and voltage-dependent current that was partially closed at a holding potential of −80 mV and slowly activated on application of 20 seconds depolarizing steps between −70 and +80 mV (Fig. 1). After repolarization to −80 mV, the current rapidly deactivated. The steady state current-voltage relationship was outwardly rectifying and showed an apparent reversal potential of ~−4 mV. These properties resembled those of Cx46 hemichannels expressed in *Xenopus* oocytes.[4] This current was present in nearly every fiber cell that was tested, although the extent of channel activation at negative potentials varied between cells. In addition, the current tended to run down during prolonged recordings. The amplitude of the current (measured at the end of a 20 seconds pulse to 80 mV) was linearly correlated to fiber cell length and cell capacitance (Fig. 2).

To measure the reversal potential and deactivation kinetics, a two-pulse protocol was used. The channels were first depolarized to 80 mV for 1.5 seconds to activate most of the channels and then repolarized to different test potentials as illustrated in Figure 3A. Figure 3B shows the instantaneous I–V curve determined by plotting the peak amplitude of the tail current as a function of voltage during the test pulse. The value of reversal potential was estimated to be −5.8 mV in this experiment. The time course of decay of the tail currents could be described by a monoexponential process. The values for the time constants of deactivation were plotted as a function of test potential in Figure 3C. The time course of deactivation became faster at more negative potentials.

In some of the smaller fibers, only a few channels were observed. These cells were suitable for studying single hemichannels. Figure 4 shows an example of a family of current traces recorded from a cell that contained only a small number of channels. At negative potentials, it was possible to measure discrete current jumps corresponding to the opening and closing of single hemichannels. The average size of these current jumps was 13 pA at −54 mV, which corresponded to a single channel conductance (γ_o = 241 pS). In 4 fiber cells, the mean value of γ_o was 243 ± 6.5 pS, which fell into approximately the same range as that previously reported for Cx46 hemichannels in transfected HeLa cells using the whole cell patch clamp technique under ionic conditions similar to those used in our study.[27] A feature that distinguishes Cx46 hemichannels from other large, nonselective channels such as pannexins is that they are inhibited by external divalent cations.[28] Figure 5 shows families of current traces and corresponding steady state I–V relationships recorded from differentiating fibers isolated from KOCx50 mouse lenses in the absence and presence of external divalent cations. Application of 1 mM $[Ca^{2+}]_o$ caused a large reduction in current amplitude and shifted the threshold of activation to more positive potentials.

If the large currents observed in divalent cation-free Ringer's solution are due to Cx46 hemichannel opening, then dye influx by gap junctional/hemichannel permeable dyes should be measurable in the fiber cells. Furthermore, dye uptake should be inhibited by agents known to block Cx46 hemichannels such as calcium, Gd^{3+}, and FFA.[29–31] Figure 6 shows an example of dye uptake measurements in a KO Cx50 fiber cell. To measure dye influx, we used the positively charged dye, propidium iodide (PrI) which has a molecular weight of 415 D and two positive charges. In the absence of external calcium, the fiber

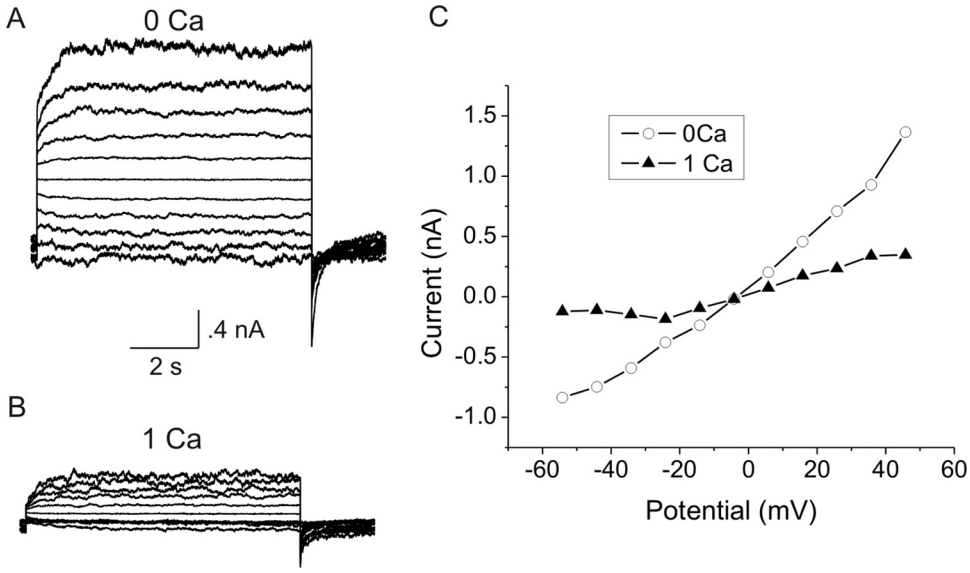

FIGURE 5. Effect of divalent cations. (**A**, **B**) Families of current recorded from a lens fiber cell before (**A**) and after (**B**) application of divalent cations. The voltage clamp protocol consisted of sequential steps from a holding potential of −60 mV to 50 mV in 10 mV increments. The membrane potential was continuously held at −60 mV between the two trials. (**C**) Isochronal I–V relationship (measured at the end of the pulse) before (*open circles*) and after (*solid triangles*) application of divalent cations.

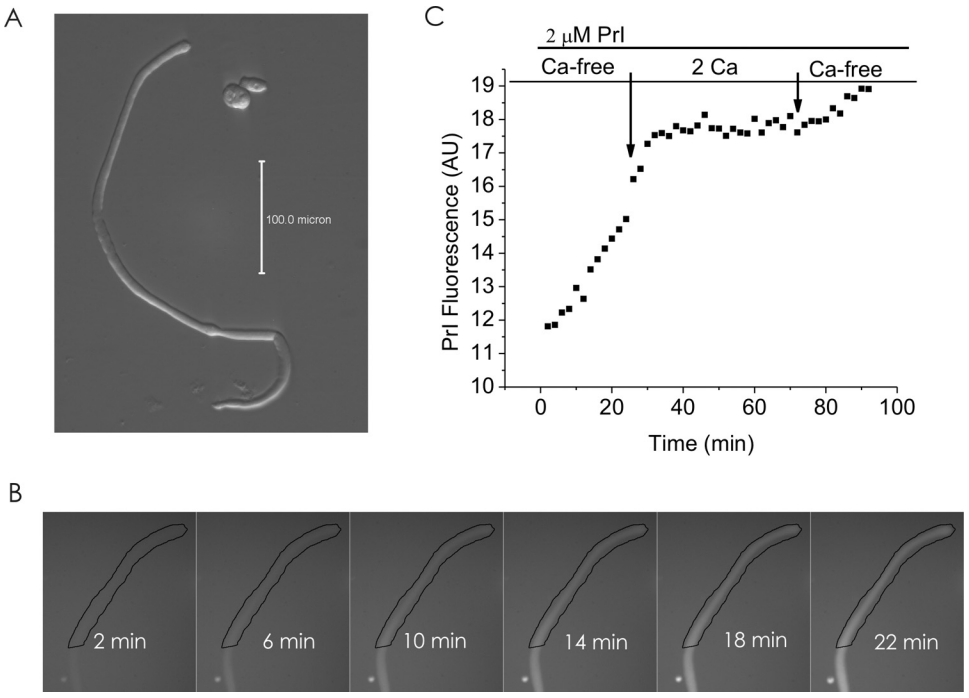

Figure 6. Dye uptake in a differentiating fiber cell isolated from the lens of a knockout Cx50 mouse. (**A**) Hoffmann image of the fiber cell used in the dye uptake experiment. (**B**) PrI images at different time points of a time-lapse recording. The cell was exposed to PrI (2 μM) starting at time 0. (**C**) Dye uptake was decreased by raising $[Ca^{2+}]_o$. To measure changes in the rate of dye uptake over time, the integrated fluorescence intensity from the ROI shown in (**B**) is plotted as a function of time in arbitrary units (a.u.). The cell was initially bathed in nominally divalent cation-free solution. At the time indicated by the *first arrow*, the cell was exposed to a solution containing 2 mM $[Ca^{2+}]_o$. Calcium was washed out at the time indicated by the *second arrow*. All the solutions contained PrI (2μM).

cell showed a linear increase in PrI fluorescence. Application of 2 mM $[Ca^{2+}]_o$ resulted in greater than 90% inhibition of dye uptake. After washout of calcium, dye uptake partially recovered. Similar results were obtained when DAPI was used to measure dye uptake. Application of 250 μM Gd^{3+}, 300 μM FFA, or 3 mM octanol also caused reductions in dye uptake. Figure 7 summarizes the effect of each of these agents on dye uptake. Gadolinium was the most potent of these blockers. At a concentration of 250 μM, Gd^{3+} inhibited greater than 95% of dye uptake. Dye uptake could also be blocked consistently by 2 mM $[Ca^{2+}]_o$. In contrast, 300 μM FFA or 3 mM octanol exhibited weaker and more variable effects.

To confirm that the calcium-sensitive conductance and dye influx were due to Cx46 hemichannels, we studied fiber cells isolated from the lenses of double KO ($Cx46^{-/-}$; $Cx50^{-/-}$) mice. In agreement with results previously reported by Xia et al.,[32] double KO lenses displayed severe cataracts but the peripheral fiber cells remained healthy. We were able to successfully isolate peripheral fiber cells from double KO lenses using the same approach that we used for the KOCx50 lenses.

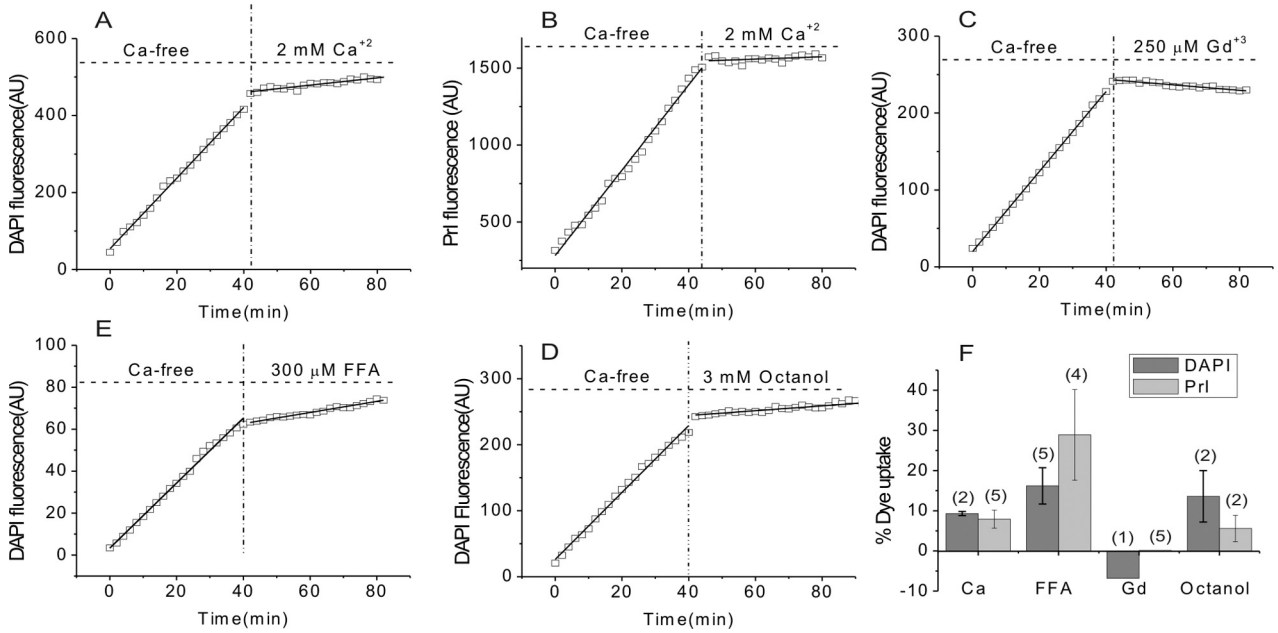

Figure 7. The rate of DAPI and PrI uptake are reduced by agents known to block connexin hemichannels. (**A–E**) Selected examples that illustrate changes in rate of DAPI and/or PrI uptake by KOCx50 fiber cells after exposure to 2 mM calcium (**A**, **B**), 250 μM gadolinium (**C**), 300 FFA μM (**D**), or 3 mM octanol (**E**). (**F**) Averaged data of effects (normalized as percent of rate of uptake in control solution) of calcium, FFA, gadolinium, and octanol on rate of uptake of DAPI (*dark gray bars*) and PrI (*light gray bars*) by KOCx50 fibers. The number of cells is indicated in parentheses.

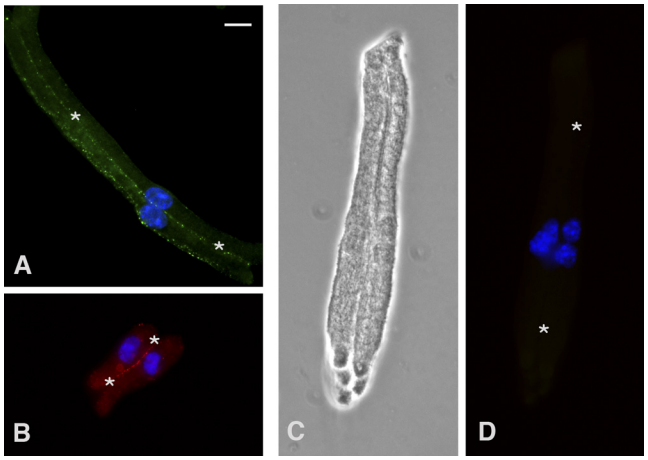

FIGURE 8. Immunolocalization of Cx46 and Cx50 in lens fiber cells collected from adult knockout mice. (**A**) Cx50 localizes along the plasma membrane between lens fiber cells from KOCx46 mice. (**B**) Cx46 localizes along the membranes between lens fiber cells from KOCx50 mice. (**C**, **D**) Lens fiber cells from Cx46, Cx50 double KO mice, shown by phase microscopy, exhibit no immunoreactivity for Cx46 or Cx50. Regions of plasma membrane apposition are indicated by *asterisks* and DAPI-stained nuclei are seen in all merged images (**A**, **B**, **D**).

The deletion of Cx50 and Cx46 was confirmed by immunohistochemical analysis of dissociated fiber cells from the double KO lenses (Fig. 8). As expected, Cx46 and Cx50 were absent in the double KO, whereas fibers from KOCx46 and KOCx50 mouse lenses showed substantial immunolocalized Cx50 and Cx46, respectively, in regions of cell apposition.

Table 1 compares the membrane properties of fiber cells isolated from double KO and KO Cx50 mouse lenses. Only fibers greater than ~50 μm in length, corresponding to a cell capacitance >25 pF, were included in this analysis. The specific conductance of the double KO fiber cells ranged from 1.4 to 16.7 pS/pF. Raising external calcium from 0 mM to 1 mM had no significant effect on membrane conductance. In contrast, fiber cells isolated from KOCx50 mouse lenses were extremely leaky in zero added calcium and had a mean specific conductance of 187.9 ± 153.6 pS/pF at a holding potential of 0 mV. Increasing external calcium caused most of the hemichannels to close, thus resulting in a reduction in membrane conductance to values comparable to those measured in double KO fibers.

Figures 9A, 9B show examples of whole-cell current traces and corresponding steady state I–V relationships recorded from a double KO fiber. Unlike KO Cx50 fiber cells, the connexin-deficient cells showed little or no channel activity when studied under calcium-free conditions. No large currents with properties resembling those of Cx46 hemichannels were detected. Figure 9C plots steady state current (measured at the end of an 8-second pulse to 80 mV) versus cell capacitance for double KO cells (closed circles) and KO Cx50 cells (open squares). The area specific steady state current at 80 mV was significantly smaller for the double KO cells (Fig. 9D).

We also evaluated dye uptake by double KO fiber cells. Figure 10 shows the average time course of uptake of PrI by KO Cx50 and double knockout fiber cells under divalent cation free conditions and after addition of 2 mM calcium. KOCx50 fibers showed robust dye uptake that could be blocked by 2 mM calcium. In contrast, double KO fiber cells showed little or no dye uptake. The PrI dye intensity measured at 40 min was on average 8x higher in KOCx50 fibers compared to double KO fibers.

DISCUSSION

Our results strongly support the hypothesis that lens fiber cells express functional Cx46 hemichannels that can be activated by depolarization or removal of external calcium.

These channels occurred ubiquitously in freshly dissociated, differentiating fiber cells. Even short cells, measuring <50 μm in length, exhibited some Cx46 hemichannel activity. Consistent with the electrophysiological data, immunofluorescent localization of Cx46 in isolated lens cells demonstrated anti-Cx46 immunoreactivity in cells as short as 20 μm in length. We feel that it is unlikely that this current represents an artifact induced by the cell dissociation procedure since a similar calcium-sensitive conductance has been observed in the intact lens.[23]

Interestingly, fiber cells that were deficient in both Cx46 and Cx50 showed little or no channel activity under conditions designed to minimize contamination by choride and potassium currents. The area-specific conductances of these cells were extremely low, having values comparable to those previously determined by whole lens impedance analysis.[33] These results suggest that connexin hemichannels may provide a pathway for influx of calcium and sodium in fiber cells. Under normal conditions, the amount of calcium and sodium entering the fiber cells would be expected to be small since Cx46 hemichannels have a low probability of opening at negative potentials in the presence of 1 mM $[Ca^{2+}]_o$. Nevertheless, this pathway may be sufficient to account for most of the sodium influx in the lens since the fiber cell sodium conductance has been estimated to be very low under physiological conditions.[34] When fiber cells are studied under conditions that enhance connexin hemichannel activity, their opening would be expected to trigger a complex sequence of events including loss of membrane potential, disruption of transmembrane ion gradients, and entry of calcium ions, followed by decreased metabolic activity (and loss of cytoplasmic ATP), activation of intracellular proteases and fiber cell death.

One situation in which enhanced hemichannel activity may occur is during fiber cell isolation. Fiber cells, when isolated in the presence of physiological concentrations of calcium, rapidly vesiculate into a series of right-side-out vesicles.[35–37] The mechanisms underlying this process have been investigated in

TABLE 1. Membrane Properties of Fiber Cells Isolated from Double KO and KOCx50 Mouse Lenses

					pS/pF	
Mouse Strain	**$[Ca^{2+}]_o$ (mM)**	**Specific Conductance* (pS/pF)**	**SE**	***n***	**Minimum**	**Maximum**
dKO	0	7.42988	2.411	6	1.5638	14.85
dKO	1	9.57655	1.754	10	1.4491	16.6667
KOCx50	0	187.88197	28.52	29	26.2985	615.2332
KOCx50	1	11.78272	1.24	16	5.3706	20.2634

* Specific conductance was measured at holding potential of 0 mV.

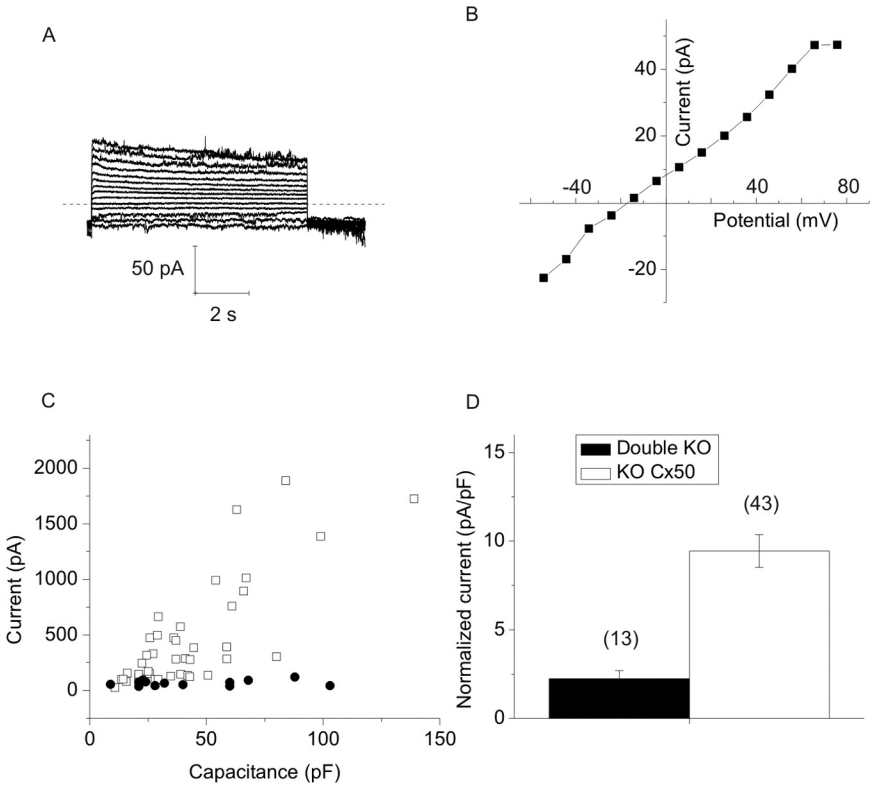

FIGURE 9. Loss of Cx50 and Cx46 abolishes calcium-sensitive membrane currents in single fiber cells. (**A**) Example of membrane currents recorded from a double KO fiber in divalent cation-free NaGluconate Ringer's solution. The voltage clamp protocol consisted of sequential steps from a holding potential of −60 mV to 80 mV in 10 mV increments. *Dashed line*: zero current. (**B**) I–V relations obtained from the data shown in (**A**). The current was measured at the end of the 8-second pulse and plotted as a function of voltage. (**C**) Steady state current (measured at the end of an 8-second pulse to 80 mV) plotted as a function of membrane capacitance for the double KO cells (*solid circles*) and the KOCx50 cells (*open squares*). (**D**) Histogram compares the mean area-specific current of the double KO cells (*open bar*) and the KOCx50 cells (*black bar*). The area-specific current was calculated from the data shown in (**C**), assuming an area-specific membrane capacitance of 1 $\mu F/cm^2$. Number of cells is indicated in parentheses.

detail in a series of studies by Bhatnager and co-workers[37–42] who showed that fiber cell globalization was associated with an increase in intracellular calcium $[Ca^{2+}]_I$, leading to an activation of intracellular proteases. This process could be slowed down or prevented by lanthanum, which blocks calcium uptake, BAPTA-AM, which buffers intracellular calcium, or removal of external chloride, which prevents Donnan swelling. Gadolinium, an irreversible blocker of connexin hemichannels and nonselective, stretch-activated cation channels, has also been shown to effectively inhibit fiber cell vesiculation.[43] A similar process occurs in diabetic cataracts where fiber cells accumulate sorbitol, which in turn induces osmotic swelling under isotonic conditions.[44]

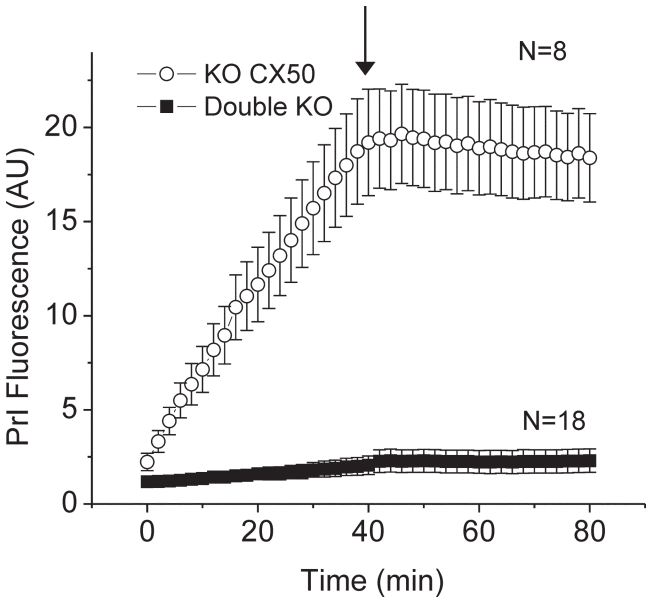

FIGURE 10. PrI uptake is reduced in fibers isolated from double KO lenses. The kinetics of PrI uptake by KOCx50 cells (*open circles*) and double KO cells (*solid circles*); each curve is the average of the fluorescence intensity from several ROI positioned on different fiber cells plotted as a function of time (normalized to fluorescence intensity at $T = 0$). The cells were initially bathed in nominally divalent cation-free solution. At the time indicated by the *arrow*, the cells were exposed to a solution containing 2 mM $[Ca^{2+}]_o$. Number of cells is indicated in parentheses.

Enhanced hemichannel activity may also be responsible for some forms of inherited cataract. Recently, we identified a novel heterozygous "gain of hemichannel mutation", hCx50G46V, in a child with an early onset total cataract.[45] Expression of hCx50G46V in *Xenopus* oocytes or HeLa cells had a deleterious effect on cell growth and/or survival. The dependence of hCx50G46V-induced cell death on hemichannel activity was suggested by the survival of *Xenopus* oocytes at increased extracellular concentrations of Ca^{2+}.

SUMMARY

Our results verify the existence of Cx46 hemichannels in isolated lens fiber cells. These channels may serve as a pathway for entry of sodium and calcium in the lens. Additional studies are needed to define the relative contribution of hemichannels versus purinergic receptor signaling and other sodium or nonselective cation channels during both physiological and pathophysiological conditions.

Acknowledgments

The authors thank Xiaoqin Liu and Tina Wadhwa for their assistance during the initial stages of this project, and the Werner Straus Live Cell Imaging Support Laboratory for fluorescence imaging studies.

References

1. Willecke K, Eiberger J, Degen J, et al. Structural and functional diversity of connexin genes in the mouse and human genome. *Biol Chem.* 2002;38361:725–737.
2. Ebihara L. New roles for connexons. *News Physiol Sci.* 2003;18: 100–103.
3. DeVries SH, Schwartz EA. Hemi-gap-junction channels in solitary horizontal cells of the catfish retina. *J Physiol.* 1992;44561:201–230.
4. Ebihara L, Steiner E. Properties of a nonjunctional current expressed from a rat connexin46 cDNA in Xenopus oocytes. *J Gen Physiol.* 1993;10261:59–74.
5. Pfahnl A, Dahl G. Gating of Cx46 gap junction hemichannels by calcium and voltage. *Pflugers Arch.* 1999;43761:345–353.
6. Paul DL, Ebihara L, Takemoto LJ, Swenson KI, Goodenough DA. Connexin46, a novel lens gap junction protein, induces voltage-gated currents in nonjunctional plasma membrane of Xenopus oocytes. *J Cell Biol.* 1991;11561:1077–1089.
7. White TW, Bruzzone R, Goodenough DA, Paul DL. Mouse Cx50, a functional member of the connexin family of gap junction proteins, is the lens fiber protein MP70. *Mol Biol Cell.* 1992;361:711–720.
8. Shiels A, Mackay D, Irisawa H, Berry V, Moore A, Bhattacharya S. A missense mutation in the human connexin50 gene (GJA8) underlies autosomal dominant "Zonular Pulverulent" cataract, on chromosome 1q. *Am J Hum Genet.* 1998;6261:526–532.
9. Berry V, Mackay D, Khaliq S, et al. Connexin 50 mutation in a family with congenital "zonular nuclear" pulverulent cataract of Pakistani origin. *Hum Genet.* 1999;10561:168–170.
10. Mackay D, Ionides A, Kibar Z, et al. Connexin46 Mutations in autosomal dominant congenital cataract. *Am J Hum Genet.* 1999; 6461:1357–1364.
11. Gong X, Li E, Klier G, et al. Disruption of a_3 connexin gene leads to proteolysis and cataractogenesis in mice. *Cell.* 1997;9161:833–843.
12. Baldo G, Gong X, Martinez-Wittingham FJ, Kumar NM, Gilula NB, Mathias RT. Gap junctional coupling in lenses from alpha(8) connexin knockout mice. *J Gen Physiol.* 2001;11861:447–456.
13. White TW, Bruzzone R, Wolfram S, Paul DL, Goodenough DA. Selective interactions among the multiple connexin proteins expressed in the vertebrate lens: the second extracellular domain is a determinant of compatibility between connexins. *J Cell Biol.* 1994;12561:879–892.
14. Ebihara L, Xu X, Oberti C, Beyer EC, Berthoud VM. Co-expression of lens fiber connexins modifies hemi-gap-junctional channel behavior. *Biophys J.* 1999;7661:198–206.
15. Ebihara L, Liu X, Pal JD. Effect of external magnesium and calcium on human connexin46 hemichannels. *Biophys J.* 2003;8461:277–286.
16. Trexler EB, Bennett MV, Bargiello TA, Verselis VK. Voltage gating and permeation in a gap junction hemichannel. *Proc Natl Acad Sci USA.* 1996;9361:5836–5841.
17. Beahm DL, Hall JE. Hemichannel and junctional properties of connexin 50. *Biophys J.* 2002;8261:2016–2031.
18. Hopperstad MG, Srinivas M, Spray DC. Properties of gap junction channels formed by Cx46 alone and in combination with Cx50. *Biophys J.* 2000;7961:1954–1966.
19. DeRosa AM, Mui R, Srinivas M, White TW. Functional characterization of a naturally occurring Cx50 truncation. *Invest Ophthalmol Vis Sci.* 2006;47:4474–4481.
20. Srinivas M, Costa M, Gao Y, Fort A, Fishman GI, Spray DC. Voltage dependence of macroscopic and unitary currents of gap junction channels formed by mouse connexin50 expressed in rat neuroblastoma cells. *J Physiol.* 1999;51761:673–689.
21. Srinivas M, Kronengold J, Bukauskas FF, Bargiello TA, Verselis VK. Correlative studies of gating in Cx46 and Cx50 hemichannels and gap junction channels. *Biophys J.* 2005;88:1725–1739.
22. Eckert R. pH gating of lens fibre connexins. *Pflugers Arch.* 2002; 443:843–851.
23. Rae JL, Mathias RT, Cooper K, Baldo G. Divalent cation effects on lens conductance and stretch-activated cation channels. *Exp Eye Res.* 1992;55(1)61:135–144.
24. Eckert R, Donaldson P, Goldie K, Kistler J. A distinct membrane current in rat lens fiber cells isolated under calcium-free conditions. *IOVS.* 1998;3961:1280–1285.
25. White TW, Goodenough DA, Paul DL. Targeted ablation of connexin50 results in micropthalmia and zonular pulverulent cataracts. *J Cell Biol.* 1998;14361:815–825.
26. White TW. Unique and redundant connexin contributions to lens development. *Science.* 2002;29561:319–320.
27. Valiunas V, Weingart R. Electrical properties of gap junction hemichannels identified in transfected HeLa cells. *Pflugers Arch.* 2000;44061:366–379.
28. Ma W, Hui H, Pelegrin P, Surprenant A. Pharmacological characterization of pannexin-1 currents expressed in mammalian cells. *J Pharmacol Exp Ther.* 2009;328:409–418.
29. Bruzzone R, Barbe MT, Jakob NJ, Monyer H. Pharmacological properties of homomeric and heteromeric pannexin hemichannels expressed in Xenopus oocytes. *J Neurochem.* 2005;92:1033–1043.
30. Eskandari S, Zampighi GA, Leung DW, Wright EM, Loo DD. Inhibition of gap junction hemichannels by chloride channel blockers. *J Membr Biol.* 2002;185:93–102.
31. Ebihara L, Steiner E. Connexin46 forms gap junctional hemichannels in Xenopus oocytes. In: Hall JE, Zampighi GA, Davis RM, eds. *Gap Junctions.* Amsterdam: Elsevier Science; 1993:75–77.
32. Xia CH, Cheng C, Huang Q, et al. Absence of alpha3 (Cx46) and alpha8 (Cx50) connexins leads to cataracts by affecting lens inner fiber cells. *Exp Eye Res.* 2006;83:688–696.
33. Baldo GJ, Mathias RT. Spatial variations in membrane properties in the intact rat lens. *Biophys J.* 1992;63(2)61:518–529.
34. Mathias RT, Kistler J, Donaldson P. The lens circulation. *J Membr Biol.* 2007;216:1–16.
35. Pasquale LR, Mathias RT, Austin LR, Brink PR, Ciunga M. Electrostatic properties of fiber cell membranes from the frog lens. *Biophys J.* 1990;58:939–945.
36. Miller AG, Zampighi GA, Hall JE. Single-membrane and cell-to-cell permeability properties of dissociated embryonic chick lens cells. *J Membr Biol.* 1992;128:91–102.
37. Bhatnagar A, Ansari NH, Wang L, Khanna P, Wang C, Srivastava SK. Calcium-mediated disintegrative globulization of isolated ocular lens fibers mimics cataractogenesis. *Exp Eye Res.* 1995;61:303–310.
38. Wang L, Bhatnagar A, Ansari NH, Dhir P, Srivastava SK. Mechanism of calcium-induced disintegrative globulization of rat lens fiber cells. *Invest Ophthalmol Vis Sci.* 1996;37:915–922.
39. Wang LF, Dhir P, Bhatnagar A, Srivastava SK. Contribution of osmotic changes to disintegrative globulization of single cortical fibers isolated from rat lens. *Exp Eye Res.* 1997;65:267–275.
40. Srivastava SK, Wang LF, Ansari NH, Bhatnagar A. Calcium homeostasis of isolated single cortical fibers of rat lens. *Invest Ophthalmol Vis Sci.* 1997;38:2300–2312.
41. Wang L, Christensen BN, Bhatnagar A, Srivastava SK. Role of calcium-dependent protease(s) in globulization of isolated rat lens cortical fiber cells. *Invest Ophthalmol Vis Sci.* 2001;42:194–199.
42. Chandra D, Ramana KV, Wang L, Christensen BN, Bhatnagar A, Srivastava SK. Inhibition of fiber cell globulization and hyperglycemia-induced lens opacification by aminopeptidase inhibitor bestatin. *Invest Ophthalmol Vis Sci.* 2002;43:2285–2292.
43. Webb KF, Merriman-Smith BR, Stobie JK, Kistler J, Donaldson PJ. Cl- influx into rat cortical lens fiber cells is mediated by a Cl-conductance that is not ClC-2 or -3. *Invest Ophthalmol Vis Sci.* 2004;45:4400–4408.
44. Reddy VN, Lin LR, Giblin FJ, Chakrapani B, Yokoyama T. Study of the polyol pathway and cell permeability changes in human lens and retinal pigment epithelium in tissue culture. *Invest Ophthalmol Vis Sci.* 1992;33:2334–2339.
45. Minogue PJ, Tong JJ, Arora A, et al. A mutant connexin50 with enhanced hemichannel function leads to cell death. *Invest Ophthalmol Vis Sci.* 2009;50:5837–5845.